# Sequential activation and distinct functions for distal and proximal modules within the IgH 3′ regulatory region

Armand Garot[a,1], Marie Marquet[a,b,1], Alexis Saintamand[a], Sébastien Bender[a,c], Sandrine Le Noir[a], Pauline Rouaud[a,2], Claire Carrion[a], Zéliha Oruc[a], Anne-Gaëlle Bébin[a,3], Jeanne Moreau[a], Kevin Lebrigand[d], Yves Denizot[a], Frederick W. Alt[e,f], Michel Cogné[a,g], and Eric Pinaud[a,4]

[a]Contrôle de la Réponse Immune B et des Lymphoprolifératıons, UMR 7276, Centre National de la Recherche Scientifique, Université de Limoges, 87025 Limoges, France; [b]Service de Néphrologie, Centre Hospitalier Universitaire Dupuytren, F-87042 Limoges, France; [c]Centre de Référence des Amyloses, Centre Hospitalier Universitaire Dupuytren, F-87042 Limoges, France; [d]Université Nice Sophia Antipolis, Centre National de la Recherche Scientifique, Institut de Pharmacologie Moléculaire et Cellulaire, 06560 Valbonne Sophia-Antipolis, France; [e]Program in Cellular and Molecular Medicine, Howard Hughes Medical Institute, Boston, MA 02115; [f]Department of Genetics, Boston Children's Hospital, Harvard Medical School, Boston, MA 02115; and [g]Institut Universitaire de France, Université de Limoges, 87000 Limoges, France

Edited by Tasuku Honjo, Graduate School of Medicine, Kyoto University, Kyoto, Japan, and approved January 6, 2016 (received for review July 23, 2015)

**As a master regulator of functional Ig heavy chain (IgH) expression, the IgH 3′ regulatory region (*3′RR*) controls multiple transcription events at various stages of B-cell ontogeny, from newly formed B cells until the ultimate plasma cell stage. The IgH *3′RR* plays a pivotal role in early B-cell receptor expression, germ-line transcription preceding class switch recombination, interactions between targeted switch (S) regions, variable region transcription before somatic hypermutation, and antibody heavy chain production, but the functional ranking of its different elements is still inaccurate, especially that of its evolutionarily conserved quasi-palindromic structure. By comparing relevant previous knockout (KO) mouse models (*3′RR* KO and *hs3b-4* KO) to a novel mutant devoid of the *3′RR* quasi-palindromic region (*3′PAL* KO), we pinpointed common features and differences that specify two distinct regulatory entities acting sequentially during B-cell ontogeny. Independently of exogenous antigens, the *3′RR* distal part, including *hs4*, fine-tuned B-cell receptor expression in newly formed and naïve B-cell subsets. At mature stages, the *3′RR* portion including the quasi-palindrome dictated antigen-dependent locus remodeling (global somatic hypermutation and class switch recombination to major isotypes) in activated B cells and antibody production in plasma cells.**

immunoglobulin gene regulation | enhancers | B-cell development

Immunoglobulin heavy chain (IgH) expression is critical for B-cell development and survival. In developing B-lineage cells, accessibility to the major remodeling events [VDJ recombination, somatic hypermutation (SHM), class switch recombination (CSR), and locus suicide recombination] depends on epigenetic changes and germ-line transcription of many regions, including $V_H$ promoters, *I*/switch region promoters, *cis*-regulatory region enhancers, and chromatin insulators (1–3). A focus on knockout (KO) models for IgH *cis*-regulatory regions (enhancers and chromatin insulators) is a means to simplify the regulation picture. At the preproB stage, the IgH locus undergoes long-range looping in a "rosette-like" structure that brings into close proximity major *IgH* regulatory regions, such as the $V_H$ to $D_H$ intergenic control regions (*IGCR1* and *-2*), the *Eμ* intronic enhancer, the 3′ regulatory region (*3′RR*), and the *3′IgH* CTCF-binding elements (*CBEs*) (4–6). Initiation of VDJ recombination is assisted by the *Eμ* enhancer, which provides efficient transcription and accessibility to initiate $D_H$ to $J_H$ rearrangements (7–10), as well as the *IGCR1* and *-2* elements that ordinate the $V_H$ to $DJ_H$ second recombination step (5, 11–13). Devoid of enhancer activity (14, 15), *3′CBE* (*hs5* to *hs8*) likely participate in *IgH* folding before VDJ recombination because deletion of *hs5* to *-7* only impacts use of proximal $V_H$ regions (16). In pre-B cells, once a functional H chain is expressed as a component of the pre–B-cell recptor (BCR), the *Eμ* enhancer function switches from $DJ_H$ region accessibility to Ig*μ* chain expression, and consequently modulates pre-BCR expression and expansion of the pre–B-cell compartment (17, 18). The activity of *Eμ* even extends to the newly formed (NF)/immature stage, where it tunes BCR expression and influences B-cell fate (18). The *3′RR* has been proven to be dispensable for locus contraction and VDJ recombination (19, 20). Its transcriptional activity starts after the pre-B stage and continues throughout B-cell development (21). The large window of activity of the *3′RR* implies that its regulatory function shifts sequentially to modulate the expression of functional H chains (in BCR-expressing cells or plasma cells), the production of germ-line regulatory transcripts correlated with Ag-dependent remodeling events, such as CSR, SHM (for review, see ref. 1), or even suicide recombination (3). The multiple KO and transgenic models developed to study *3′RR* function (21) have brought considerable information, although quite puzzling, given that models have been mostly studied individually. Transgenic models carrying bacterial artificial chromosomes prohibit B-cell development and chromatin studies but provided information on CSR and SHM (22).

## Significance

**The immunoglobulin heavy chain (IgH) 3′regulatory region (*3′RR*) fine-tunes *IgH* gene expression during B cell development. One singularity of this region is its quasi-palindromic structure conserved in the *3′RR* of other species. By comparing previous mouse knockout (KO) models (*3′RR*- and *hs3b-4* KO) to a novel mutant devoid of the quasi-palindrome (*3′PAL* KO), we highlighted common features and differences that specify two distinct regulatory entities: (*i*) the distal module (*hs4*) is sufficient for normal IgH expression up to the naïve B cell stage; (*ii*) during B-cell activation, the proximal module (quasi-palindrome) is important for both class switch recombination and somatic hypermutation; and (*iii*) in plasma cells, the quasi-palindrome is required for robust transcription of the IgH locus.**

Author contributions: A.G., M.M., A.-G.B., F.W.A., M.C., and E.P. designed research; A.G., M.M., A.S., S.B., S.L.N., P.R., C.C., A.-G.B., and E.P. performed research; A.G., M.M., A.S., S.B., C.C., Z.O., K.L., Y.D., and E.P. contributed new reagents/analytic tools; A.G., M.M., A.S., S.L.N., P.R., C.C., K.L., F.W.A., M.C., and E.P. analyzed data; and A.G., M.M., A.S., J.M., M.C., and E.P. wrote the paper.

The authors declare no conflict of interest.

This article is a PNAS Direct Submission.

Data deposition: The data reported in this paper have been deposited in the Gene Expression Omnibus (GEO) database, www.ncbi.nlm.nih.gov/geo (accession no. GSE76217).

[1]A.G. and M.M. contributed equally to this work.

[2]Present address: SILAB R&D, 19240 Saint-Viance, France.

[3]Present address: Center for Vaccine and Immunology, University of Georgia, Athens, GA 30602.

[4]To whom correspondence should be addressed. Email: eric.pinaud@unilim.fr.

This article contains supporting information online at www.pnas.org/lookup/suppl/doi:10.1073/pnas.1514090113/-/DCSupplemental.

Taking CSR into account, bacterial artificial chromosome transgene studies point out a cumulative activity of *IgH 3′* enhancer elements, with special activities for some of them, such as *hs1-2*, *hs4* alone or combined with *hs3b* (23, 24), and on the other hand, exonerate any effect of the *hs3* homologs (25). Transgenic models contradict endogenous deletion studies with regards to BCR expression and antibody secretion (23). From endogenous deletion models, we learned that *3′RR* enhancers share redundant functions because individual KOs had no significant consequences on B-cell remodeling events (26–28), whereas combined deletion of *hs3b* and *hs4* decreased CSR to all isotypes, except for IgG1 (29). The entire *3′RR* deletion demonstrates the potency of the region at all steps: deficient mice cumulate BCR-expression defects (30), global SHM defects (31), abrogated CSR, and failure to secrete Igs (32).

Another singularity of the *3′RR* is its quasi-palindromic structure centered around *hs1-2*, composed of inverted repeats for about 25 kb and terminating by virtually identical *hs3a* and *hs3b* enhancers in the mouse (33, 34). A similar quasi-palindromic organization is conserved in the *3′RR* of other species, including humans and apes (3, 35, 36). Strikingly, evolution did not conserve virtual homology of *3′RR* inverted regions but preserved its global structure. Such a selection implies a dedicated function for the *3′RR* quasi-palindrome that has not yet been elucidated. Our present study describes and compares a new KO mouse model devoid of the quasi-palindromic *3′RR* proximal module (*3′PAL* KO) to relevant models (Fig. 1) lacking the distal module (*hs3b-4* KO) (29) or the entire region (*3′RR* KO) (32). Common features and differences raised by this side-by-side comparison reveal that the *3′RR* is composed of two functional entities that activate sequentially during B-cell development.

## Results

**Deletion of the Proximal *IgH 3′RR* Module in the Mouse.** To determine the role of the "proximal *3′RR* structural module" (Fig. 1) (called "*3′PAL*" for *IgH* 3′ quasi-palindromic region), we introduced a *loxP-pTK-neo$^R$-loxP* cassette in place of the 26.4-kb region that includes *hs3a*, *hs1-2*, and *hs3b* enhancers by homologous recombination into 129/Ola ES cells (Fig. S1*A*). Once introduced into the mouse germ line, the selection cassette was deleted, as described previously (18), to get the *3′PAL$^\Delta$* model (Fig. S1*B*). Our study used either homozygous mutant mice (of mixed background, predominantly 129) or F1 heterozygous mice obtained after breeding to *wt* C57BL/6 mice. We compared *3′PAL* deletion to previous models devoid of the two distal *3′IgH* enhancers (*hs3b-4$^\Delta$*) (29) or the entire *3′RR* (*3′RR$^\Delta$*) (32).

**The Distal *3′RR* Module (*hs4*) Is Sufficient for Antigen-Independent B-Cell Ontogeny (from PreproB to Naïve B Cells).** Because the *hs4* enhancer remains upon our *3′PAL* deletion, this mouse KO strain is a model of choice to evaluate the function of the *3′RR* distal module in developing B cells. To avoid any disparity linked to the murine genetic background (30, 37), the antigen-independent phase of B-cell development was assessed in mouse models carrying IgH alleles of distinct allotypes. In such models, IgM-allotype expression in developing B-lineage cells reflects competition between the "b" allotype IgH *wt* allele (from C57BL/6 mice) and the "a" allotype IgH mutant allele (from 129 mice). We compared bone marrow and spleen B-lineage cell subsets of *wt* F1 mice (*IgH$^{wta/wtb}$*) to models carrying heterozygous deletions of the IgH *3′RR* modules: proximal module (this study, *3′PAL$^{\Delta a/wtb}$*), distal *hs3b* and *hs4* elements (*hs3b-4$^{\Delta a/wtb}$*), and the complete *3′RR* (*3′RR$^{\Delta a/wtb}$*). We combined surface staining with intracellular IgM-allotype staining to precisely determine, in each relevant cell subset, both the proportion (and the resulting ratio) of IgM$^a$ or IgM$^b$-expressing cells and the mean fluorescence of each IgM-allotype (and its ratio). Disruption of part or the entire *3′RR* did not compromise early B-cell development because all four models displayed similar numbers and proportions of IgM$^a$- or IgM$^b$-expressing cells in the bone marrow NF/immature B-cell subset (Fig. 2, Fig. S2, and Table S1). Even though a slight decrease in expression of the mutated allele (IgM$^a$) had already been seen in NF B cells from *3′RR$^{\Delta a/wtb}$* and *hs3b-4$^{\Delta a/wtb}$* animals (Fig. 2), this had no consequence on the inflow of NF B cells. Deletion of the proximal *3′RR* module had no effect on developing B-lineage cells: *3′PAL$^{\Delta a/wtb}$* animals displayed normal numbers and proportions of all bone marrow and spleen B-cell subsets (Fig. S2), most likely the consequence of normal IgM$^a$ heavy chain expression in these cells (Fig. 2). This theory was confirmed in homozygous *3′PAL$^{\Delta/\Delta}$* mice harboring B-cell compartments comparable to *wt* mice (Table S2).

**The Distal *3′RR* Module (*hs4*) Is Required for Efficient BCR Expression in Transitional B Cells.** Deletion of the proximal *3′RR* module strongly contrasted with *3′IgH*-deletions that encompass the distal *hs4* element: in the spleen of *3′RR$^{\Delta a/wtb}$* and *hs3b-4$^{\Delta a/wtb}$* animals, numbers and proportions of splenic transitional B cells expressing IgM$^a$ allele was decreased (Fig. 2, Fig. S2, and Table S1). This disadvantage in the generation of transitional B cells was correlated with decreased expression (about twofold compared with *wt* cells, as evaluated by mean fluorescence intensity) of the IgM$^a$ mutated allele (Fig. 2). This result was associated with a decrease in numbers and proportions of IgM$^a$-expressing mature B-lineage cells: marginal zone (MZ) and follicular (FO) B cells from the spleen, mature recirculating B cells in the bone marrow, and B1 cell subsets in the peritoneal cavity in *3′RR$^{\Delta a/wtb}$* and *hs3b-4$^{\Delta a/wtb}$* animals (Fig. 2, Fig. S2, and Table S1). Deletion of either proximal, distal, or the entire *3′RR* showed marked differences on Ig heavy chain expression in developing B cells. A locus devoid of the distal module (*3′RR$^\Delta$* and *hs3b-4$^\Delta$*) failed to express a normal amount of surface Ig$\mu$ heavy chain (already observed in NF B cells) with drastic consequences on the capacity to generate mature naïve B-cell subsets. On the other hand, our *3′PAL* KO model proved that the *hs4* enhancer was per se sufficient to drive efficient expression of $\mu$ heavy chain in developing B cells.

**The Proximal *3′RR* Module Drives Germ-Line Transcription and CSR to *γ1*, *γ3*, and *γ2a* Genes.** Global IgH locus transcriptional activation was assessed by comparing RNA-seq data obtained from resting and in vitro LPS-activated splenic B cells from *wt* and homozygous *3′PAL*, *hs3b-4*, and *3′RR* KO animals. If sense and antisense germ-line transcripts (GLT) for the whole locus were above background in *3′RR* KO B cells, deletions of distal and proximal *3′RR* modules led to intermediate levels of *IgH* GLT upon LPS activation (Fig. 3 and Fig. S3). Compared with wt cells, induction of sense GLT in the *γ3* region was decreased in all KO models, whereas GLT of the $\mu$ region was not affected by *hs3b-4* deletion. In contrast, *γ2b* region GLT were still normally induced in *3′PAL*-deficient B cells (Fig. 3). To more precisely evaluate the function of the proximal *3′RR* on CSR, splenic B cells from *wt* and homozygous *3′PAL* KO mice were subjected to appropriate in vitro stimulations and tested for switched BCR expression and GLT (Fig. S4 *A* and *B*). B cells deficient for the quasi-palindrome displayed a significant CSR defect to IgG3, IgG1, and IgG2a isotypes (reduced by two- to threefold). This finding was correlated with a consistent defect in GLT of both

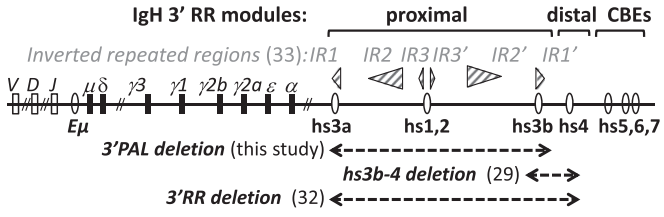


**Fig. 1.** The *IgH 3′RR*: structure and KO mouse models. Mouse IgH locus showing details of genomic regions across the *3′RR*. Horizontal triangles represent inverted repeated regions forming a quasi-palindrome. Deletions carried out in the mouse models used for the study are indicated (see introductory paragraphs for details).

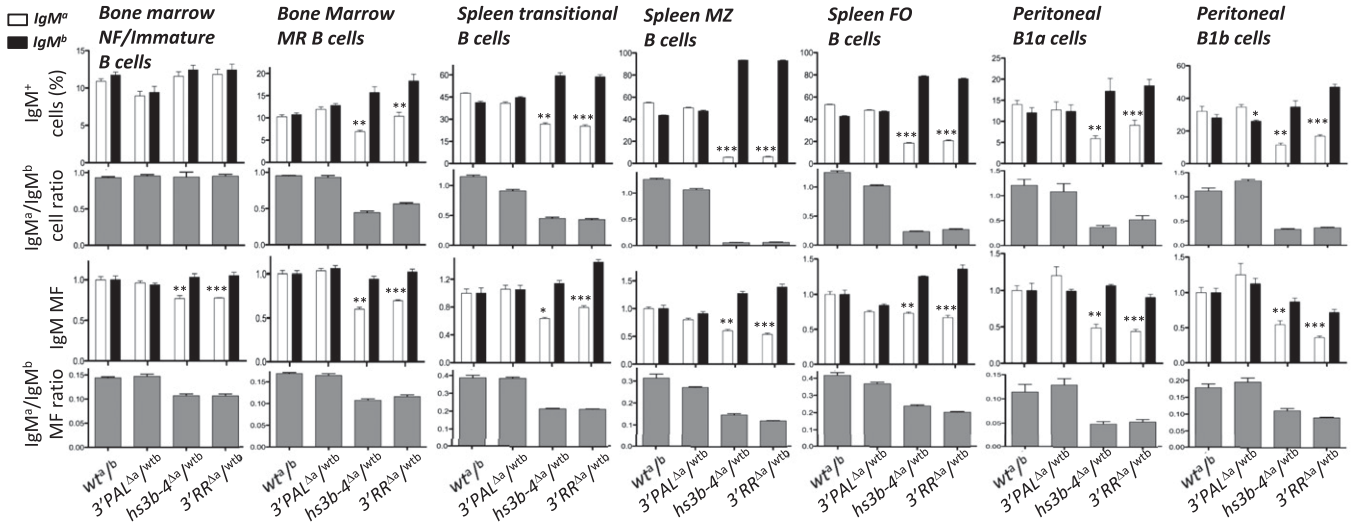


**Fig. 2.** Normal IgM-expressing naïve B-cell subsets require the *3′RR* distal module. B-lineage cell subsets in heterozygous models: $wt^{a}/^{b}$, $3'PAL^{\Delta a}/^{wtb}$, $hs3b\text{-}4^{\Delta a}/^{wtb}$, and $3'RR^{\Delta a}/^{wtb}$. Bone marrow NF/immature and mature recirculating (MR) B cells; spleen transitional, MZ, and FO B cells; peritoneal cavity B1a and B1b subsets were analyzed by flow cytometry as described in Fig. S2. Top histograms display percentages of $IgM^{a}$ (white) or $IgM^{b}$ (black) expressing cells; gray histograms below reported the corresponding ratio. Bottom histograms give intracellular $IgM^{a}$ or $IgM^{b}$ allotype mean fluorescence (MF), gray histograms below report the corresponding MF ratio. Cell numbers were collected from five to seven animals of each genotype. Significant differences were indicated by *P* values: $*P < 0.05$, $**P < 0.01$, $***P < 0.001$ according to the Mann–Whitney *u* test.

donor and acceptor switch regions (Fig. S4*A*) in $3'PAL^{\Delta/\Delta}$: *Iγ3-Cγ3* GLT was reduced by fivefold; *Iμ-Cμ*, *Iγ1-Cγ1*, and *Iγ2a-Cγ2a* GLT were reduced by threefold. In contrast to complete *3′RR* deletion (32), in vitro CSR to IgG2b and IgA was not significantly reduced by the deletion of the proximal *3′RR* region (Fig. S4*B*) and their corresponding germ-line transcripts were detected in almost normal proportions in stimulated $3'PAL^{\Delta/\Delta}$ B cells (Fig. S4 *A* and *B*). Decreased Ig secretion of all isotypes in supernatants of $3'PAL^{\Delta/\Delta}$-stimulated cells (Fig. S4*C*) was a feature shared with the *3′RR* deletion, suggesting, beyond an isotype-specific CSR defect, a global Ig secretion defect (*Discussion*). As potential targets of the *IgH 3′RR*, we determined expression of the recently described long-noncoding RNA (lncRNA) associated with CSR (38) and found, based on RNA-seq, no variation in all models in resting or LPS-activated B cells (Fig. 3). This finding was confirmed by quantitative RT-PCR (qRT-PCR) experiments showing that *wt* and *3′PAL*-deficient B cells (resting or stimulated) displayed same amounts of lncRNA-CSR transcripts (Fig. S4*D*).

**The Proximal *3′RR* Module Controls SHM in a Transcription-Dependent Manner.** SHM was assayed in GC B cells ($B220^{+}/PNA^{High}/FAS^{+}$) sorted from Peyer's patches of *wt* and homozygous $3'PAL^{\Delta/\Delta}$ animals. At the IgH locus, SHM frequency in the ∼500-bp intronic regions downstream from rearranged-$J_H3$ or -$J_H4$ segments was reduced by-threefold in $3'PAL^{\Delta/\Delta}$ GC B cells (0.005 mutations per base pair) compared with *wt* (0.014 mutations per base pair) (Fig. 4*A*). When comparing the distribution of mutated sequences, we found that $3'PAL^{\Delta/\Delta}$ GC B cells were largely unmutated (72%), whereas *wt* control had only a small proportion (7%) of unmutated cells (Fig. 4*A*). Mutated *IgH* alleles from GC B cells devoid of the proximal module contained only few mutations (27% of sequences, with fewer than six substitutions). Similarly to the whole *3′RR* deletion (31), highly mutated *IgH* alleles (>six mutations) were almost absent in our *3′PAL* mutants (Fig. 4*A*). As a control experiment, SHM was also quantified in the intron downstream from the *Jκ5* segment and found both the mutation frequency and the percentage of mutated sequences to be comparable with that in *wt* (Fig. 4*A*). We finally quantified *IgH* primary transcription by qRT-PCR with a probe downstream from the $J_H4$ intron and found a two- to threefold reduction in CG B cells lacking the proximal module (Fig. 4*B*). In naïve B cells ($B220^{+}/PNA^{low}/FAS^{-}$) sorted from Peyer's patches, *IgH* primary transcription levels were similar in *wt* and $3'PAL^{\Delta/\Delta}$ mice, confirming that the *3′RR* proximal module did not modulate heavy chain expression in resting B cells.

**Plasma Cell Antibody Production and the Antigen-Specific Responses Rely on the *3′RR* Proximal Module.** The first evidence of Ig secretion defects in animals lacking the *3′RR* distal module was the drastic reduction of all circulating Ig, including IgM, in the serum of $3'PAL^{\Delta/\Delta}$ mice (Fig. S5*A*). This hypogammaglobulinemia was similar to that previously observed in *3′RR* KO mice (32). When challenged with ovalbumin, heterozygous $3'PAL^{\Delta a}/^{wtb}$ mutants proved that a deficient allele was unable to support efficient antibody production (Fig. S5*B*). The $IgM^{a}$-specific response was consistently decreased (Fig. S5*B*), whereas $IgG1^{a}$ and $IgG2a^{a}$ responses were completely abrogated (Fig. S5*B*), probably the consequence of combined CSR and Ig secretion defects. Plasma cell differentiation and ability to produce Ig was then evaluated in heterozygous mice after intraperitoneal challenge with sheep red blood cells. All models showed efficient generation of plasma cells expressing both $IgM^{a}$ and $IgM^{b}$ allotypes in the spleen 6 d after challenge (Fig. 4*C*). Remarkably, plasma cells carrying *IgH* alleles devoid of the proximal module ($3'PAL^{\Delta}$ and $3'RR^{\Delta}$ alleles) exhibited a strong defect in intracellular IgM expression (Fig. 4*D*). To look for the origin of the defect, *IgH* transcription was assayed in resting and in vitro-activated B cells from homozygous *3′PAL* KO mice. In this plasmablast-enriched population, both the *IgH* primary and the secreted form of the *μ* chain transcripts were drastically reduced in the absence of the proximal module (Fig. 4*E*).

## Discussion

There is no doubt that the *3′RR* plays a key role in IgH locus regulation (39) but the role of the conserved quasi-palindrome and the hierarchy between the modules remained poorly understood. By comparing relevant KO mouse models, our study demonstrated that the *3′RR* includes at least two functional modules: (*i*) the distal module, which includes the *hs4* enhancer element; and (*ii*) the proximal module, defined as the *3′RR* quasi-palindrome. First, independently of antigen stimuli, we confirmed that VDJ recombination does not require any of the *3′RR* enhancers. In all models, early B-cell development was preserved, with normal pro– and pre–B-cell compartments. This finding correlates with studies proving normal VDJ rearrangements and $V_H$ use in such models (19, 40). Second, our study identifies the

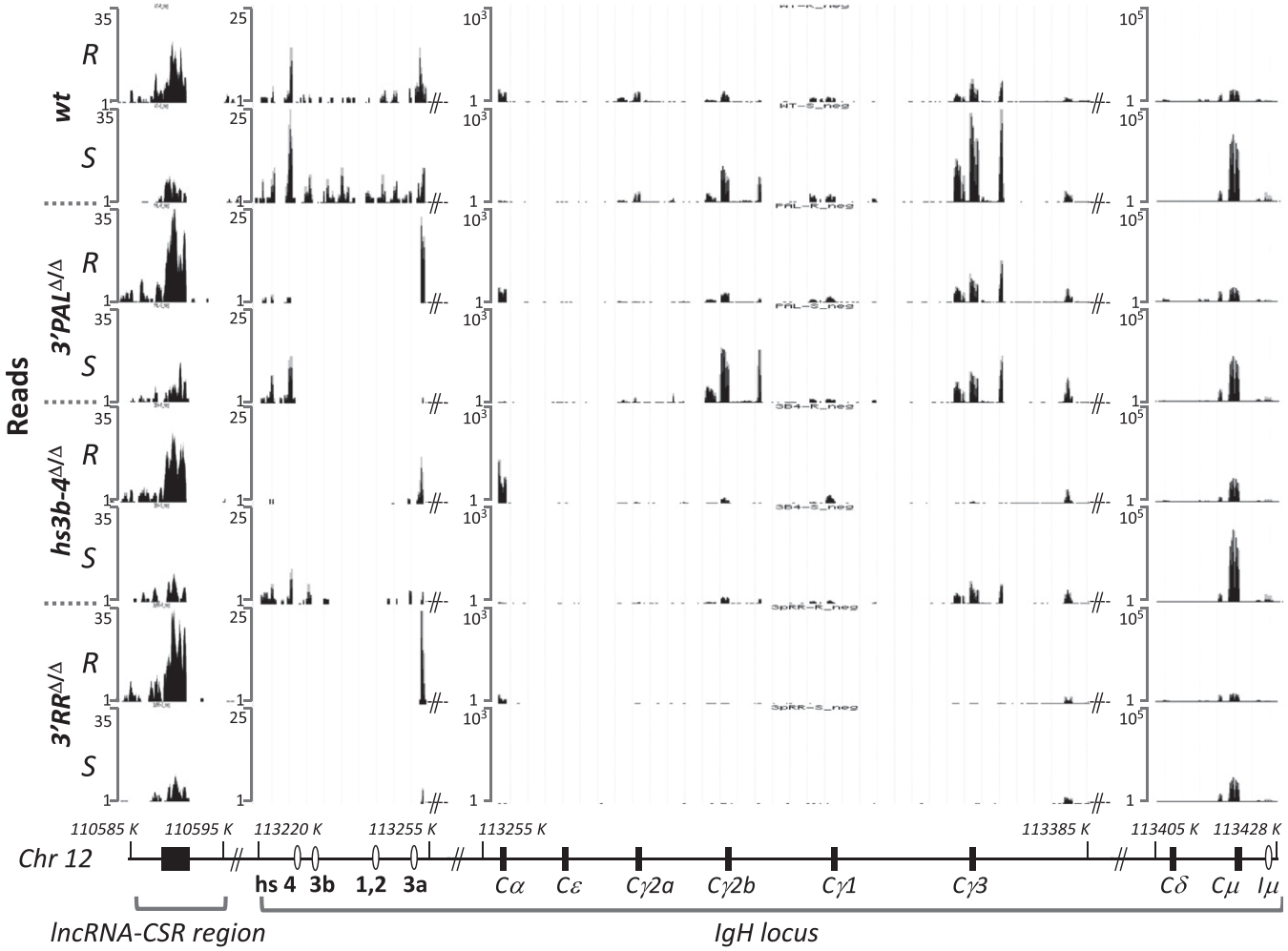


**Fig. 3.** Varigated induction of *IgH*-associated transcripts upon *3′RR* deletions. Expression of sense transcripts at the IgH locus based on RNA-seq read distribution in resting B cells sorted from the spleen (R) and LPS-activated B cells for 48 h (S) from *wt*, *3′PAL*$^{\Delta/\Delta}$, *hs3b-4*$^{\Delta/\Delta}$, and *3′RR*$^{\Delta/\Delta}$ mice. Each RNA-seq experiment was performed on a pool of equivalent numbers of B cells sorted from four age-matched animals of the same genotype. Reads were aligned on mouse GRCm38/mm10 assembly using University of California, Santa Cruz Genome Browser (49), base position on mouse Chr12 are reported. A map of the IgH locus (not to scale), including constant genes, regulatory elements, and orientation of the reported transcripts is indicated.

critical role of the distal *3′RR* module for Ig heavy chain expression in a defined window starting as soon as a complete BCR is expressed (NF B cells) and extending until the naïve B-cell stage. In B-lineage precursors, a first contribution was assigned to CBEs, which have been proposed to facilitate interactions between locus distant regions (14, 20, 41, 42). Deletion of *hs5-7* CBEs downstream from the mouse *3′RR* resulted in only a slight modification of *D* and $V_H$ use (16), suggesting a modest contribution of 3′ CBEs in VDJ joining, although it is not excluded that full deletion (including *hs8*) might have a more drastic effect (39). Once VDJ recombination is completed, the *3′RR* and the promoter of the VDJ-rearranged segment continue to interact and then starts the actual *3′RR* stepwise transcriptional activation by its distal module. Indeed, when developing B cells were driven by IgH alleles lacking the *hs4* distal enhancer (*hs3b-4*$^{\Delta}$ or *3′RR*$^{\Delta}$), a progressive decrease in μH-chain expression was already observed in NF B cells (about 30% decrease at this stage compared with *wt*, based on IgM$^a$/IgM$^b$ mean fluorescence ratio) and rose to a 50% decrease in transitional B cells. Such "low BCR-expressing" NF and transitional B cells displayed a differentiation disadvantage (observed in both models devoid of *hs4*) toward mature MZ and FO B-cell subsets. In the *3′PAL* KO model, normal Igμ expression in bone marrow NF B cells and spleen mature B subsets clearly shows the proximal *3′RR* module as dispensable at these stages. These findings pinpoint the window of activity for the distal module and support a stepwise activation of the *IgH 3′RR*: *hs4* is required to maintain optimal μ heavy chain transcription from the NF bone marrow to the mature MZ and FO splenic B cells. This window of activity clearly overlaps with that of *Eμ*, recently described as active on μH-chain transcription from pre-B to transitional B-cell stages (18).

When mature B cells encounter antigen and engage in an immune response, the *3′RR* proximal module takes over most of IgH locus regulatory mechanisms: SHM, CSR, and antibody production. First, SHM seems strongly dependent on the proximal module. The drastic reduction in SHM frequency in germinal center (GC) B cells from *3′PAL*$^{\Delta/\Delta}$ mice (0.005 mutations per base pair downstream from the $J_H$ introns, excluding unmutated sequences) was similar to that observed in *3′RR*-deficient animals (31), a model described as deficient for recruiting activation-induced cytidine deaminase (AID) in *IgH* variable regions (43). In our *3′PAL*$^{\Delta}$ mice, the SHM defect was also correlated with a decrease (at least twofold) in *IgH* primary transcription, a defect comparable to that seen in *3′RR*-deficient mice (31). The *IgH* transcription defect in *3′PAL*-deficient GC B cells also provides further evidence that *hs4* does not influence H-chain expression once B cells are activated. Even if such a twofold transcription decrease appears modest, it is certainly significant.

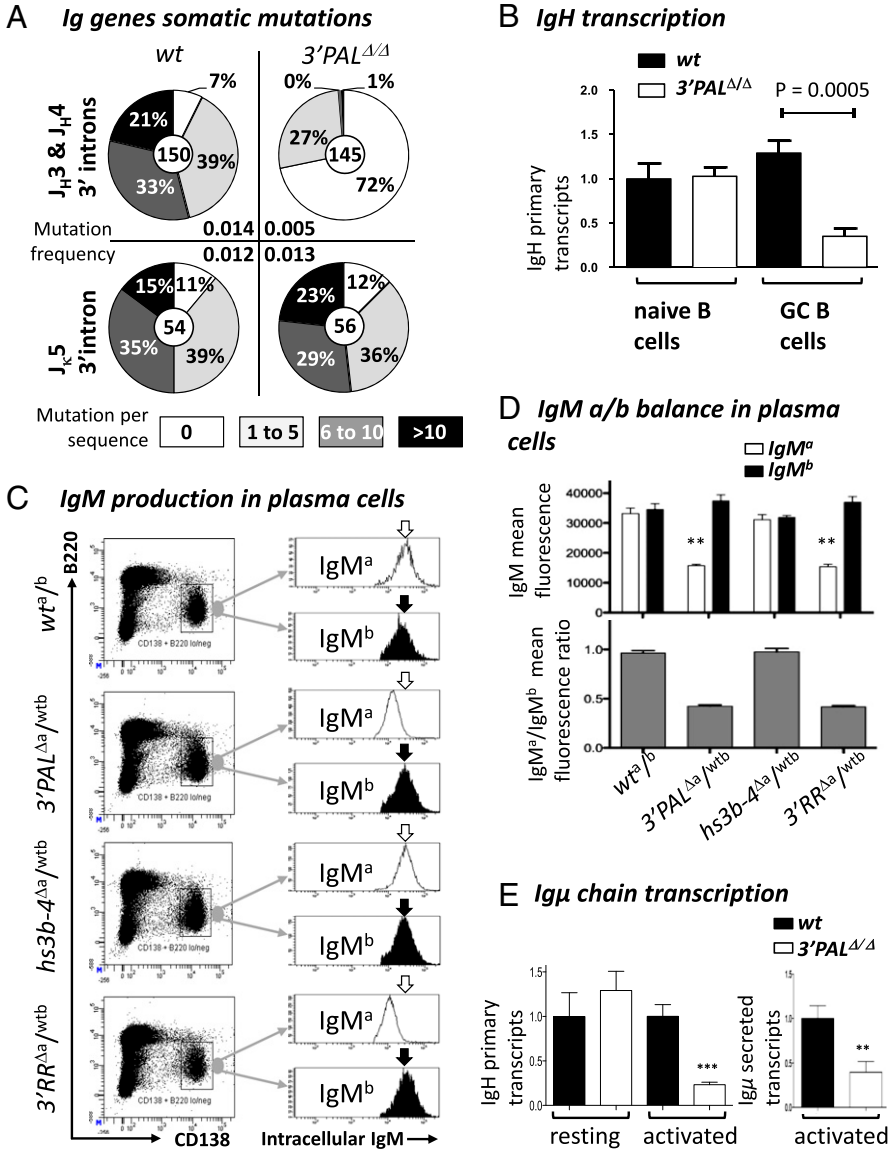


**Fig. 4.** Proximal *3′RR* module controls *IgH* somatic mutations in GC B cells and Ig production in plasma cells. (*A*) GC B-cell DNA was isolated from B220$^{+}$ PNA$^{high}$/FAS$^{high}$ Peyer's patch cells from unimmunized 8-wk-old *wt* and *3′PAL* KO mice. Pie plots showed the percentage of mutated clones for each group (proportional to the area in each slice).Total number of clones analyzed for each genotype was noted in the center. Mutation frequency (mutation per base pair, indicated for each group) was calculated from sequences that contained at least one mutation; clonally related sequences were excluded. (*B*) Relative *IgH* primary transcripts was estimated by qRT-PCR, performed using *IgH*$^{wt}$ TaqMan probe and normalized to *Cd79a* transcripts (see Table S3 for details). (*C*) Intracellular IgM-allotype expression in plasma cells from heterozygous mouse models (*wt*$^{a}$/$^{b}$; *3′PAL*$^{\Delta a}$/$^{wtb}$, *hs3b-4*$^{\Delta a}$/$^{wtb}$, and *3′RR*$^{\Delta a}$/$^{wtb}$) was measured by FACS analysis. After sheep red blood cell challenge, plasma cells from the spleen were gated based on surface expression of B220$^{low}$ and CD138$^{+}$. This specific population was assayed for intracellular expression of IgM$^{a}$ or IgM$^{b}$ allotypes. One representative experiment is shown. (*D*) *Upper* histogram shows mean fluorescence of intracellular IgM$^{a}$ (white) or IgM$^{b}$ (black) allotype expression (estimated by flow cytometry as described above) in plasma cells collected from at least five animals of each genotype. Gray histograms below report the corresponding MF IgM$^{a}$/IgM$^{b}$ ratio. (*E*) *IgH* primary and secreted-Ig$\mu$ transcripts in *wt* and *3′PAL*$^{\Delta/\Delta}$ B cells. (*Left*) Primary transcription of rearranged *IgV*$_{H}$ regions (normalized to *Gapdh* transcripts) was quantified by qRT-PCR in CD43$^{-}$ resting B cells from *wt* and *3′PAL*$^{\Delta/\Delta}$ animals). (*Right*) Transcription of the secreted form of Ig $\mu$ heavy chain was quantified by qRT-PCR (see Table S3 for details). Significant differences were indicated by *P* values: $^{**}P < 0.01$, $^{***}P < 0.001$ according to the Mann–Whitney *u* test.

Indeed, it is admitted that the level of BCR expression modulates B-cell fate and that a basal level of H-chain transcription is necessary for B-cell survival (44). Besides a similar transcription defect in both models, the proportion of unmutated sequences (72%) in *3′PAL*-deficient GC B cells was, however, lower than in *3′RR*-KO mice (95%) (31). Even if *hs4* does not impact transcription at this stage, its partnership with the *3′PAL* module for AID recruitment or targeting can be suspected in light of the higher proportion of unmutated *IgH* alleles in *3′RR* KO than in *3′PAL*-deficient mice. Second, germ-line transcription of major switch regions is regulated by the proximal *3′RR* module. Transcription of the donor *Sμ* region is decreased by at least threefold in *3′PAL*-deficient B cells induced for CSR in vitro (32, 45); the same is true for GLT of *Sγ3*, *Sγ1*, and *Sγ2a* acceptor switch regions, two features shared with the *3′RR*-KO model (32). The failure of a *3′PAL*-deficient allele to support IgG1- or IgG2a-specific responses is also consistent with a CSR defect. Interestingly, the *3′PAL*$^{\Delta/\Delta}$ phenotype preserved normal GLT and CSR to IgG2b and IgA, whereas these processes were affected in animals lacking both *hs3b* and *hs4* enhancers or the entire *3′RR* (29, 32). Specifying that *hs4* is by itself sufficient for normal GLT and CSR to *Cγ2b* and *Cα*, our study underlined the complexity of constant gene transcriptional regulation for CSR.

Among potential regulatory mechanisms involving the *3′RR*, the lncRNA for CSR, recently described in the CH12 cell line undergoing CSR to IgA, promotes the CSR-stimulating activity of the *3′RR* via a long-distance interaction with the *hs4* region (38). It is possible that lncRNA-CSR (normally expressed in *3′PAL*-deficient B cells), promotes efficient CSR to IgA and IgG2b in this model that conserved the *hs4* module. Third, in plasma cells, the common feature shared by both *3′RR* and *3′PAL* deletions proved that Ig heavy chain transcription and antibody production are directly under the control of the *3′RR* proximal module.

We hypothesize that *IgH 3′RR* modules respond sequentially maybe independently to external stimuli: (*i*) the distal (*hs4*) module being responsible for efficient heavy chain and BCR expression in NF and naïve B-cell subsets, and (*ii*) the proximal quasi-palindromic module being later activated by exogenous antigen stimulation to support both SHM, CSR (with some help from *hs4* in the situation of *Sγ2b* and *Sα* CSR), and prolonged IgH overexpression in antibody secreting cells.

## Materials and Methods

**Flow Cytometry.** Once isolated from mouse organs, single-cell suspensions of bone marrow, spleen, peritoneal cavity, and Peyer's patches were labeled

with various fluorescent antibodies, as detailed in *SI Materials and Methods*. To collect plasma cells, mice were injected with 200 μL sheep red blood cell suspension (bioMérieux) in the peritoneal cavity. At day 6, mice were killed and splenic plasma cells analyzed by flow cytometry as described in *SI Materials and Methods*. All animal experiments were performed according to the guidelines of the Comité Régional d'Ethique du Limousin (CREAAL 7-07-2012 approved protocol).

**RNA Isolation and qRT-PCR.** Total RNA was isolated and RT-PCR was performed as described previously (18). TaqMan probes and primers, previously described in (9, 31, 38, 46–48), are listed in Table S3. Relative mRNA levels were normalized to *Gapdh* or *Cd79a* transcripts.

**RNA-Seq Analysis.** RNA-seq libraries were prepared from a pool of equivalent numbers of B-purified B cells, either resting B cells from the spleen or in vitro-activated B cells for 48 h with LPS, from four animals of each genotype. Sequencing and analysis are described in *SI Materials and Methods*.

**SHM.** The experimental procedures for Peyer's patch GC and naïve B cells sorting, genomic extraction, amplification, and cloning have been previously reported (9). Amplification of $VDJ_H$- or $VJ_\kappa$-rearranged DNA fragments was performed with the appropriate primers (Table S3). Mutational analysis was performed in either the 500-bp intronic region just downstream from $J_H3$ and $J_H4$ segments (for IgH locus) or in the 554-bp intronic region located downstream from the $J\kappa5$ segment (for Igκ locus).

**ACKNOWLEDGMENTS.** We thank all members of the Service Commun d'Animalerie and Plateforme de Transgenose of Limoges University for mouse work; Catherine Ouk-Martin and the FACS sorting facility of Limoges University; Drs. Laurent Delpy, Christophe Sirac, and Brice Laffleur for discussions and helpful comments; and Virginie Magnone, Alexandra Popa, and Pascal Barbry for help and fruitful discussions. This work was developed in close collaboration with the functional genomics platform of Nice Sophia Antipolis, a partner of the National Infrastructure France Génomique, thanks to support by the Cancéropôle PACA and Commissariat aux Grands Investissements (PB: ANR-10-INBS-09-03 and ANR-10-INBS-09-02). This work was supported in part by a PhD joint scholarship from Centre National de la Recherche Scientifique and Région Limousin (to M.M.); a PhD scholarship from the Région Limousin (to A.G., P.R., and A.-G.B.); a PhD scholarship from the Ministère de l'Enseignement Supérieur et de la Recherche (to A.S.); Grant DOC20150602943 from Fondation ARC (to A.S.); post doc Fellowship Grant ANR-11-BSV302701 (to S.L.N.); and grants from ARC (#SL220100601332), Conseil Régional du Limousin, Ligue Contre le Cancer, Comités de la Région Limousin, ANR-11-BSV30270, and Comité d'Orientation Recherche Cancer en Limousin.

1. Perlot T, Alt FW (2008) *Cis*-regulatory elements and epigenetic changes control genomic rearrangements of the IgH locus. *Adv Immunol* 99:1–32.
2. Sleckman BP, Oltz EM (2012) Preparing targets for V(D)J recombinase: Transcription paves the way. *J Immunol* 188(1):7–9.
3. Péron S, et al. (2012) AID-driven deletion causes immunoglobulin heavy chain locus suicide recombination in B cells. *Science* 336(6083):931–934.
4. Jhunjhunwala S, et al. (2008) The 3D structure of the immunoglobulin heavy-chain locus: Implications for long-range genomic interactions. *Cell* 133(2):265–279.
5. Guo C, et al. (2011) CTCF-binding elements mediate control of V(D)J recombination. *Nature* 477(7365):424–430.
6. Choi NM, Feeney AJ (2014) CTCF and ncRNA regulate the three-dimensional structure of antigen receptor loci to facilitate V(D)J recombination. *Front Immunol* 5:49.
7. Afshar R, Pierce S, Bolland DJ, Corcoran A, Oltz EM (2006) Regulation of IgH gene assembly: Role of the intronic enhancer and 5′DQ52 region in targeting DHJH recombination. *J Immunol* 176(4):2439–2447.
8. Bolland DJ, et al. (2007) Antisense intergenic transcription precedes IgH D-to-J recombination and is controlled by the intronic enhancer Emu. *Mol Cell Biol* 27(15):5523–5533.
9. Perlot T, Alt FW, Bassing CH, Suh H, Pinaud E (2005) Elucidation of IgH intronic enhancer functions via germ-line deletion. *Proc Natl Acad Sci USA* 102(40):14362–14367.
10. Sakai E, Bottaro A, Davidson L, Sleckman BP, Alt FW (1999) Recombination and transcription of the endogenous Ig heavy chain locus is effected by the Ig heavy chain intronic enhancer core region in the absence of the matrix attachment regions. *Proc Natl Acad Sci USA* 96(4):1526–1531.
11. Featherstone K, Wood AL, Bowen AJ, Corcoran AE (2010) The mouse immunoglobulin heavy chain V-D intergenic sequence contains insulators that may regulate ordered V(D)J recombination. *J Biol Chem* 285(13):9327–9338.
12. Giallourakis CC, et al. (2010) Elements between the IgH variable (V) and diversity (D) clusters influence antisense transcription and lineage-specific V(D)J recombination. *Proc Natl Acad Sci USA* 107(51):22207–22212.
13. Lin SG, Guo C, Su A, Zhang Y, Alt FW (2015) CTCF-binding elements 1 and 2 in the Igh intergenic control region cooperatively regulate V(D)J recombination. *Proc Natl Acad Sci USA* 112(6):1815–1820.
14. Nicolás L, Chaudhuri J (2013) 4C-ing the Igh Landscape. *Immunity* 39(2):199–201.
15. Garrett FE, et al. (2005) Chromatin architecture near a potential 3′ end of the igh locus involves modular regulation of histone modifications during B-cell development and in vivo occupancy at CTCF sites. *Mol Cell Biol* 25(4):1511–1525.
16. Volpi SA, et al. (2012) Germline deletion of Igh 3′ regulatory region elements hs 5, 6, 7 (hs5-7) affects B cell-specific regulation, rearrangement, and insulation of the Igh locus. *J Immunol* 188(6):2556–2566.
17. Li F, Eckhardt LA (2009) A role for the IgH intronic enhancer E mu in enforcing allelic exclusion. *J Exp Med* 206(1):153–167.
18. Marquet M, et al. (2014) The Eμ enhancer region influences H chain expression and B cell fate without impacting IgVH repertoire and immune response in vivo. *J Immunol* 193(3):1171–1183.
19. Rouaud P, et al. (2012) Enhancers located in heavy chain regulatory region (hs3a, hs1,2, hs3b, and hs4) are dispensable for diversity of VDJ recombination. *J Biol Chem* 287(11):8356–8360.
20. Medvedovic J, et al. (2013) Flexible long-range loops in the VH gene region of the Igh locus facilitate the generation of a diverse antibody repertoire. *Immunity* 39(2):229–244.
21. Pinaud E, et al. (2011) The IgH locus 3′ regulatory region: Pulling the strings from behind. *Adv Immunol* 110:27–70.
22. Dunnick WA, et al. (2009) Switch recombination and somatic hypermutation are controlled by the heavy chain 3′ enhancer region. *J Exp Med* 206(12):2613–2623.
23. Dunnick WA, Shi J, Zerbato JM, Fontaine CA, Collins JT (2011) Enhancement of antibody class-switch recombination by the cumulative activity of four separate elements. *J Immunol* 187(9):4733–4743.
24. Dunnick WA, Shi J, Fontaine C, Collins JT (2013) Transgenes of the mouse immunoglobulin heavy chain locus, lacking distal elements in the 3′ regulatory region, are impaired for class switch recombination. *PLoS One* 8(2):e55842.
25. Yan Y, et al. (2011) Homologous elements hs3a and hs3b in the 3′ regulatory region of the murine immunoglobulin heavy chain (IgH) locus are both dispensable for class-switch recombination. *J Biol Chem* 286(31):27123–27131.
26. Manis JP, et al. (1998) Class switching in B cells lacking 3′ immunoglobulin heavy chain enhancers. *J Exp Med* 188(8):1421–1431.
27. Vincent-Fabert C, et al. (2009) Ig synthesis and class switching do not require the presence of the hs4 enhancer in the 3′ IgH regulatory region. *J Immunol* 182(11):6926–6932.
28. Bébin A-G, et al. (2010) In vivo redundant function of the 3′ IgH regulatory element HS3b in the mouse. *J Immunol* 184(7):3710–3717.
29. Pinaud E, et al. (2001) Localization of the 3′ IgH locus elements that effect long-distance regulation of class switch recombination. *Immunity* 15(2):187–199.
30. Saintamand A, et al. (2015) The IgH 3′ regulatory region governs μ chain transcription in mature B lymphocytes and the B cell fate. *Oncotarget* 6(7):4845–4852.
31. Rouaud P, et al. (2013) The IgH 3′ regulatory region controls somatic hypermutation in germinal center B cells. *J Exp Med* 210(8):1501–1507.
32. Vincent-Fabert C, et al. (2010) Genomic deletion of the whole IgH 3′ regulatory region (hs3a, hs1,2, hs3b, and hs4) dramatically affects class switch recombination and Ig secretion to all isotypes. *Blood* 116(11):1895–1898.
33. Chauveau C, Cogné M (1996) Palindromic structure of the IgH 3′locus control region. *Nat Genet* 14(1):15–16.
34. Saleque S, et al. (1997) Dyad symmetry within the mouse 3′ IgH regulatory region includes two virtually identical enhancers (C alpha3′E and hs3). *J Immunol* 158(10):4780–4787.
35. Sepulveda MA, Garrett FE, Price-Whelan A, Birshtein BK (2005) Comparative analysis of human and mouse 3′ Igh regulatory regions identifies distinctive structural features. *Mol Immunol* 42(5):605–615.
36. D'Addabbo P, Scascitelli M, Giambra V, Rocchi M, Frezza D (2011) Position and sequence conservation in amniota of polymorphic enhancer HS1.2 within the palindrome of IgH 3′regulatory region. *BMC Evol Biol* 11:71.
37. Kaminski DA, Stavnezer J (2007) Antibody class switching differs among SJL, C57BL/6 and 129 mice. *Int Immunol* 19(4):545–556.
38. Pefanis E, et al. (2015) RNA exosome-regulated long non-coding RNA transcription controls super-enhancer activity. *Cell* 161(4):774–789.
39. Birshtein BK (2014) Epigenetic regulation of individual modules of the immunoglobulin heavy chain locus 3′ regulatory region. *Front Immunol* 5:163.
40. Morvan CL, Pinaud E, Decourt C, Cuvillier A, Cogné M (2003) The immunoglobulin heavy-chain locus hs3b and hs4 3′ enhancers are dispensable for VDJ assembly and somatic hypermutation. *Blood* 102(4):1421–1427.
41. Degner SC, et al. (2011) CCCTC-binding factor (CTCF) and cohesin influence the genomic architecture of the Igh locus and antisense transcription in pro-B cells. *Proc Natl Acad Sci USA* 108(23):9566–9571.
42. Degner SC, Wong TP, Jankevicius G, Feeney AJ (2009) Cutting edge: Developmental stage-specific recruitment of cohesin to CTCF sites throughout immunoglobulin loci during B lymphocyte development. *J Immunol* 182(1):44–48.
43. Maul RW, et al. (2014) Spt5 accumulation at variable genes distinguishes somatic hypermutation in germinal center B cells from ex vivo-activated cells. *J Exp Med* 211(11):2297–2306.
44. Lam KP, Kühn R, Rajewsky K (1997) In vivo ablation of surface immunoglobulin on mature B cells by inducible gene targeting results in rapid cell death. *Cell* 90(6):1073–1083.
45. Saintamand A, et al. (2015) Elucidation of IgH 3′ region regulatory role during class switch recombination via germline deletion. *Nat Commun* 6:7084.
46. Park S-R, et al. (2009) HoxC4 binds to the promoter of the cytidine deaminase AID gene to induce AID expression, class-switch DNA recombination and somatic hypermutation. *Nat Immunol* 10(5):540–550.
47. Park S-R, Seo G-Y, Choi A-J, Stavnezer J, Kim P-H (2005) Analysis of transforming growth factor-beta1-induced Ig germ-line gamma2b transcription and its implication for IgA isotype switching. *Eur J Immunol* 35(3):946–956.
48. Sellars M, Reina-San-Martin B, Kastner P, Chan S (2009) Ikaros controls isotype selection during immunoglobulin class switch recombination. *J Exp Med* 206(5):1073–1087.
49. Kent WJ, et al. (2002) The human genome browser at UCSC. *Genome Res* 12(6):996–1006.